Absolute Interferometric Testing of Spherical Surfaces

Bruce E. Truax, Zygo Corporation
Laurel Brook Road, Middlefield, CT 06455

ABSTRACT

In typical interferometric testing the part under test is measured against a reference standard. The measured result is the difference between the errors in the test and reference surfaces plus any additional errors introduced by the interferometer. For accurate qualification of the reference surface it is necessary to employ a technique that can measure the part absolutely. This paper examines an existing technique[1] for absolute testing of spherical surfaces which produces a map of the entire surface. The capabilities of this technique, error sources, and experimental data will be examined.

1. INTRODUCTION

It is well known that interferometry of optical surface figure is a relative measurement. An interferometer measures the difference in surface shape between the surface under test and, in the case, of a Fizeau Interferometer, the reference surface. For other interferometer configurations such as a Twyman-Green, the errors of additional optics in the cavity are also included in the measurement. For this reason the most common, commercially available interferometers are of the Fizeau configuration and they are used with high quality reference optics. Typical reference optic quality is 1/20th of a wavelength at 0.6328 μm yielding a measurement accuracy of about 1/10th wavelength. Obtaining higher accuracy measurements requires absolute surface measurement techniques. These absolute techniques are used either by the metrologist to test the surface in question or by the fabricator of the reference optic to produce and guarantee higher accuracy reference surfaces. There are two techniques available for performing absolute surface measurement. One technique is known as the 3-Flat method and is used to absolutely measure a diameter on a flat surface. The second technique, and the subject of this paper, is known as spherical surface certification and it is used to absolutely measure the entire surface of a spherical optical element.

The technique of spherical surface certification was first described by A. F. Jensen in 1973 for Twyman-Green interferometers.[2] It was later referenced in two papers. There is no published reference with the derivation of the formulae.[3],[4] This paper presents the derivation of the formulae used in this procedure as applied to a Fizeau interferometer as well as some actual test results using this technique with a commercially available interferometer.

2. THEORY

A greatly simplified schematic of a Fizeau interferometer is shown in Fig. 1.

The incoming wavefront of coherent light is assumed to have no aberration and is represented by $W_I(r,\theta)e^{i(kz+\omega t)}$. This beam passes through beam forming optics, the focusing lens, the reference surface and finally reflects from the test surface. Each of these surfaces adds aberration to the wavefront. It is assumed that the input beam and all apertures are circular and that the phase aberrations can be represented by circular polynomials of the form.

$$\vartheta(r,\theta) = \sum_{n=0}^{\infty} \sum_{m=0}^{\infty} C_{nm} r^n (\cos m\theta + \sin m\theta) \qquad (1)$$

where r is normalized to 1 at the edge of the aperture.

---

[1] Jensen, A.E., "Absolute Calibration Method for Laser Twyman-Green Wavefront Testing Interferometers," Paper ThG19, Fall OSA Meeting, Rochester, N.Y (October 1973).
[2] Ibid.
[3] Bruning, J. H., et al., "Digital Wavefront measuring Interferometer for Testing Optical Surfaces and Lenses," Applied Optics, Vol. 13 No. 11, pp. 2693-2703 (Nov. 1974) .
[4] Berman, J., Hunter, G.C., Truax, B.E., "Interferometric Lens Testing to λ/40 at λ=0.442 Microns," Presented at Optical Fabrication and Testing Conference, Cherry Hill, New Jersey (June 1985).

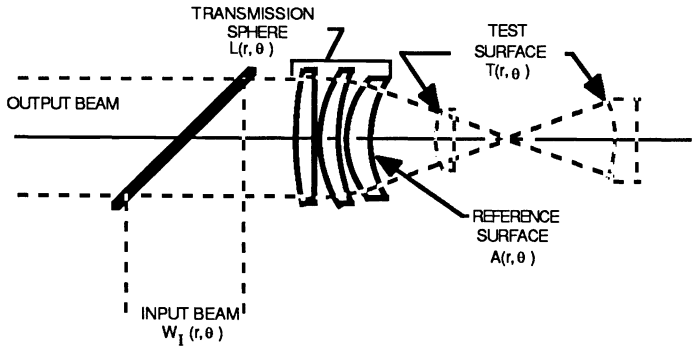

Figure 1. Interferometer Schematic

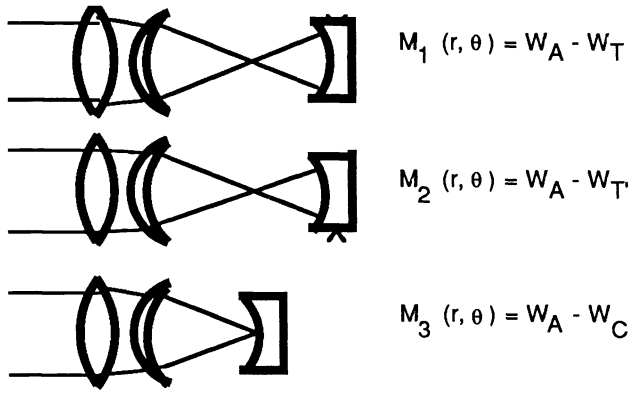

where $W_A(r,\theta)$ is the wavefront reflected from the aplanat,
$W_T(r,\theta)$ is the wavefront reflected from the test surface,
$W_{T'}(r,\theta)$ is the wavefront reflected from the test surface after 180° rotation,
$W_C(r,\theta)$ is the wavefront reflected from the cat's eye reflection.

Figure 2. Spherical Certification Measurements

The absolute measurement of the test surface T(r,θ) requires three measurements as shown in Fig. 2.

Using Figs. 1 and 2, Eq. (1), and the fact that the aberrations introduced by each element in the optical path add linearly, the results of the measurements can be calculated. First calculate each wavefront component.

$$W_A(r,\theta) = I(r,\theta) + 2\,L(r,\theta) + 2n\,A(r,\theta)\,. \tag{2}$$

$$W_T(r,\theta) = I(r,\theta) + 2\,L(r,\theta) + 2(n-1)\,A(r,\theta) + 2\,T(r,\theta)\,. \tag{3}$$

$$W'_T(r,\theta) = I(r,\theta) + 2\,L(r,\theta) + 2(n-1)\,A(r,\theta) + 2\,T(r,\theta + 180°)\,. \tag{4}$$

$$W_C(r,\theta) = I(r,\theta) + L(r,\theta) + (n-1)\,A(r,\theta) + (n-1)\,A(r,\theta + 180°) + L(r,\theta + 180°)\,. \tag{5}$$

Where $I(r,\theta)$ is the wavefront error of the source,
$L(r,\theta)$ is the wavefront error introduced by the focusing optics in the aplanat,
$A(r,\theta)$ is the error in the aplanat reference surface, and
$T(r,\theta)$ is the error in the surface under test.

Since $\cos m\theta = \cos m(\theta + 180°)$ and $\sin m\theta = -\sin m(\theta + 180°)$ for m odd, Eq. (5) can be reduced to

$$W_C(r,\theta) = I(r,\theta) + \begin{cases} 2\,L(r,\theta) + 2\,(n-1)\,A(r,\theta) & m \text{ even} \\ 0 & m \text{ odd} \end{cases} \tag{6}$$

Next, combine the wavefronts into the individual measurements.

$$M_1(r,\theta) = W_A(r,\theta) - W_T(r,\theta). \tag{7}$$

$$M_1(r,\theta) = \left[\, I(r,\theta) + 2\,L(r,\theta) + 2n\,A(r,\theta) \,\right] - \left[\, I(r,\theta) + 2\,L(r,\theta) + 2\,(n-1)\,A(r,\theta) + 2\,T(r,\theta)\right]. \tag{8}$$

$$M_1(r,\theta) = 2\,A(r,\theta) - 2T(r,\theta). \tag{9}$$

$$M_2(r,\theta) = W_A(r,\theta) - W'_T(r,\theta). \tag{10}$$

$$M_2(r,\theta) = \left[\, I(r,\theta) + 2\,L(r,\theta) + 2n\,A(r,\theta) \,\right] - \left[\, I(r,\theta) + 2\,L(r,\theta) + 2\,(n-1)\,A(r,\theta) + 2\,T(r,\theta + 180°)\right]. \tag{11}$$

$$M_1(r,\theta) = 2\,A(r,\theta) - 2T(r,\theta + 180°). \tag{12}$$

$$M_3(r,\theta) = W_A(r,\theta) - W_C(r,\theta). \tag{13}$$

$$M_3(r,\theta) = [\, I(r,\theta) + 2\,L(r,\theta) + 2n\,A(r,\theta) \,] - I(r,\theta) + \begin{cases} 2\,L(r,\theta) + 2\,(n-1)\,A(r,\theta) & m \text{ even} \\ 0 & m \text{ odd} \end{cases} \tag{14}$$

$$M_3(r,\theta) = \begin{cases} 2\,A(r,\theta) & m \text{ even} \\ 2\,L(r,\theta) + 2n\,A(r,\theta) & m \text{ odd} \end{cases} \tag{15}$$

Now that the three measurements have been made, two intermediate computations are performed. In the first computation $M_3(r,\theta)$ is added to itself after a rotation of 180°.

$$\Psi(r,\theta) = M_3(r,\theta) + M_3(r,\theta + 180°) \tag{16}$$

$$\Psi(r,\theta) = \begin{cases} 2\,A(r,\theta) + 2\,A(r,\theta + 180°) & m \text{ even} \\ 2\,L(r,\theta) + 2n\,A(r,\theta) + 2\,L(r,\theta + 180°) + 2n\,A(r,\theta + 180°) & m \text{ odd} \end{cases} \tag{17}$$

$$\Psi(r,\theta) = \begin{cases} 4\,A(r,\theta) & m \text{ even} \\ 0 & m \text{ odd} \end{cases} \tag{18}$$

The second intermediate computation is the sum of $M_1(r,\theta)$ and $M_2(r,\theta)$ after rotating $M_2(r,\theta)$ by 180°.

$$\Psi'(r,\theta) = M_1(r,\theta) + M_2(r,\theta + 180°). \tag{19}$$

$$\Psi'(r,\theta) = \left[2\,A(r,\theta) - 2\,T(r,\theta)\right] + \left[\, 2\,A(r,\theta + 180°) - 2\,T(r,\theta + 360°)\right]. \tag{20}$$

$$\Psi'(r,\theta) = -4\,T(r,\theta) + \begin{cases} 4\,A(r,\theta) & m \text{ even} \\ 0 & m \text{ odd} \end{cases} \tag{21}$$

The solution is now obvious, by taking 1/4 of the difference between Ψ and Ψ', $T(r, \theta)$ is found.

To summarize, by referring to Fig. 2 and Eqs. (16) and (19), the following formula is derived.

$$T(r,\theta) = \frac{1}{4}\left\{ \left[M_3(r,\theta) + M_3(r,\theta + 180°)\right] - \left[\, M_1(r,\theta) + M_2(r,\theta + 180°)\right] \right\} \tag{22}$$

This equation is easily implemented on phase measuring interferometers where the data is defined on a uniform grid.

3. EXPERIMENTAL RESULTS

Spherical surface certification has been implemented using a Zygo MARK IV interferometer, special software, and a precision mount. Software to implement Eq. (22) has been written using the MARK IV's programming capability. This software guides the user through the three measurements and makes provision for locating the optical axis. The precision mount, shown in Fig. 3, allows for translation of the part between the "cat's eye" and confocal positions as well as for the necessary 180° rotation of the test optic. In addition, a special reticle is provided that when used in conjunction with the software allows for accurate location of the optical axis.

Figure 4 illustrates an example of the results of this test procedure for testing an f/2 spherical surface. This same f/2 surface was measured using seven different transmission optics. A summary of the seven measurements is shown in Table 1. Note the excellent repeatability of data. The peak-to-valley errors have a spread of 0.02λ.

Meas. #	PV	rms
1	.057	.007
2	.064	.008
3	.063	.009
4	.044	.006
5	.046	.007
6	.054	.008
7	.053	.007
Std. Dev.	.008	.001

Table 1. Experimental Repeatability

This same technique has been used by the author's company to successfully fabricate and certify f/1 spherical surfaces to 0.025λ at λ=442nm.[1]

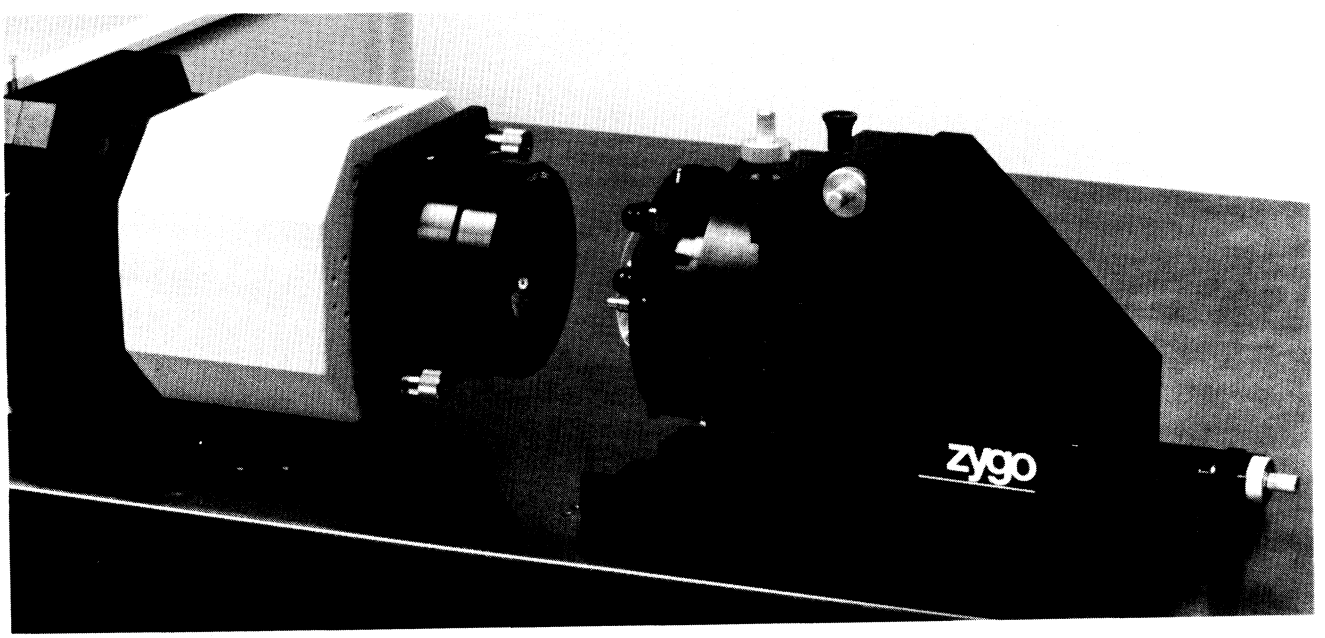

Figure 3. Photograph of Precision Mount for Spherical Surface Certification

[1] Berman, J., Hunter G.C., Truax, B.E., "Interferometric Lens Testing to λ/40 at λ=0.442 Microns'" Presented at Optical Fabrication and Testing Conference, Cherry Hill, New Jersey (June 1985).

*** CONFOCAL ***

03-AUG-1988/12: 22: 47
Part ID : CONFOCAL
Serial # : CONFOCAL
Fast : ON
Averages : 4
Trim : 0
Calibrate : ON
AGC : ON
Scale : 0.50
Wave Out : 0.6328
Remove : TLT PWR

PV : 0.106 **PTS : 22217**
RMS : 0.009

POWER : 0.0030

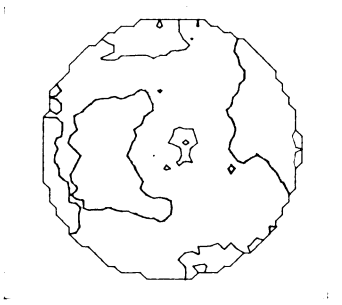

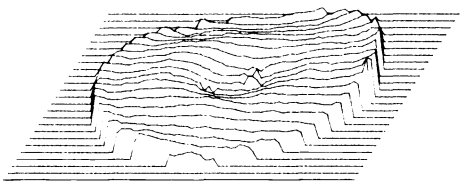

*** CONFOCAL (180) ***

03-AUG-1988/12: 31: 50
Part ID : CONFOCAL (180)
Serial # : CONFOCAL (180)
Fast : ON
Averages : 4
Trim : 0
Calibrate : ON
AGC : ON
Scale : 0.50
Wave Out : 0.6328
Remove : TLT PWR

PV : 0.123 **PTS : 22258**
RMS : 0.008

POWER : -0.0091

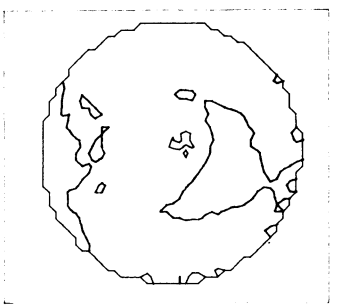

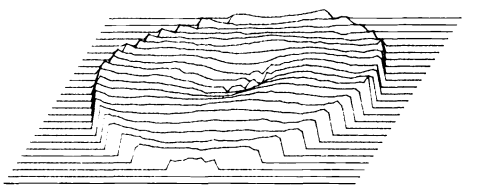

Figure 4. Experimental Results

*** CAT'S EYE ***

03-AUG-1988,/12: 19: 37
Part ID : CAT'S EYE
Serial # : CAT'S EYE
Fast : ON
Averages : 4
Trim : 0
Calibrate : ON
AGC : ON
Scale : 0.50
Wave Out : 0.6328
Remove : TLT PWR

PV : 0.096 **PTS : 30715**
RMS : 0.014

POWER : -0.0810

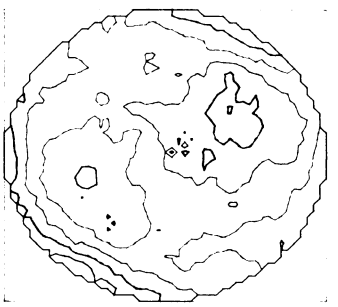

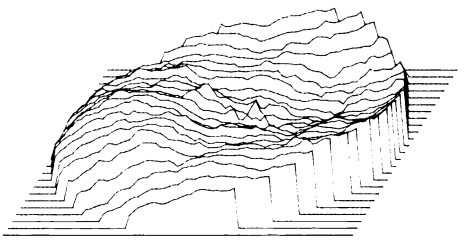

*** TEST PART ***

03-AUG-1988,/12: 19: 37
Part ID : f/2.0 TS
Serial # :
Fast : ON
Averages : 4
Trim : 0
Calibrate : ON
AGC : ON
Scale : 0.50
Wave Out : 0.6328
Reference : DEMO LAB f/.75 TS
Remove : TLT PWR

PV : 0.060 **PTS : 21707**
RMS : 0.008

POWER : 0.0390

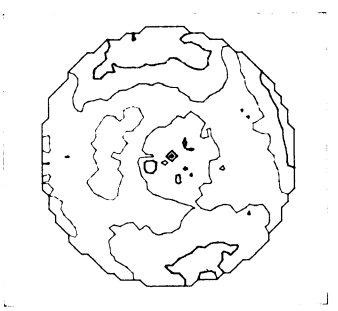

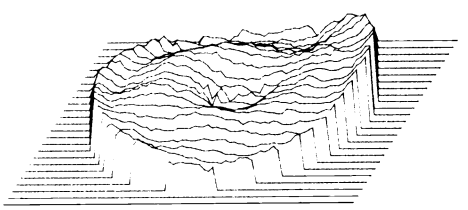

Figure 4. Experimental Results (Cont.)

4. SOURCES OF ERROR

4.1 Instrument Precision

As with any interferometric metrology vibration, thermal instability and electronic noise will cause random errors in the individual measurements that are then combined using Eq. (22) to yield the final measurement result. These errors can be minimized using proper vibration isolation and data averaging. The Zygo MARK IV instrument precision is better than 0.002λ rms for individual measurements, in a good environment. Equation (22) combines four measurements three of which are statistically independent. If the rotated "cat's eye" measurement is also considered independent for the purpose of this computation, then the resulting rms error due to these noise sources is less than 0.004λ rms.

4.2 Systematic Error

There are two sources of systematic errors that must also be considered, these are improper location of the optical axis and errors due to distortion when measuring with non-nulled interferometer cavities.

4.2.1 Optical Axis Location

Due to the data rotation that is necessary to compute the surface figure $T(r,\theta)$, proper location of the optical axis is critical if accurate results are to be obtained. Incorrect location of the optical axis causes a wavefront shear which introduces errors that are proportional to the errors present in the individual wavefronts. When testing high quality optics with a Fizeau interferometer, the measurement with the most aberration is the "cat's eye" measurement. Typically this measurement will have significant coma (all aberrations proportional to even multiples of θ cancel, see Eq. (15), except for errors in the reference surface which are usually quite small). The coma should cancel as shown in Eq. (18) when M_3 is added to itself after 180° rotation of the data. If the optical axis is located incorrectly, astigmatism will be introduced into the final result due to the lateral shear of the comatic wavefront. The magnitude of this error can be expressed as

$$\varepsilon = 3\delta C \cos\varphi \tag{23}$$

where
δ=optical axis location error expressed as a fraction of the aperture diameter
C=magnitude of 3rd order coma
φ=angle between the coma and the line formed by the table optical axis and the chosen optical axis.

As a simple example, if $\varphi=0$, $C=0.5\lambda$ and $\delta=0.005$ then $\varepsilon=0.008\lambda$ of cylinder in the final result. This is beginning to be significant when measuring surfaces with accuracies of 0.025λ.

4.2.2 Non-Nulled Interference Cavities

Deriving the optimum accuracy from any phase measuring interferometer system can only be accomplished by making measurements with nulled interference cavities. Distortion present in the interferometer imaging system will introduce errors that are proportional to the slope errors of the wavefront being measured. When testing high quality surfaces these slope errors will be minimal as long as the tests are performed with the interference cavity nulled. As an example, take the case of simple defocus when combined with third order distortion. The wavefront form for defocus is shown in Eq. (24).

$$W(r,\theta) = k\, r^2 \tag{24}$$

where k is the defocus in waves of error at the edge of the aperture.

Third order distortion introduces an error into the position coordinate r of the form

$$r = r' + \zeta\, r'^3 \tag{25}$$

where ζ is the fractional distortion at the edge of the aperture.

Substituting Eq. (25) into Eq. (24) the form of the wavefront at the detector can be derived as in Eq. (26)

$$W'(r,\theta) = k\,[\, r^2 + 2\zeta r^4 + \zeta^2 r^6]. \tag{26}$$

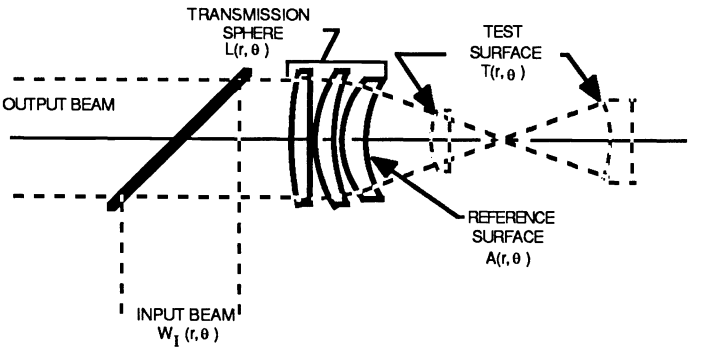

Figure 1. Interferometer Schematic

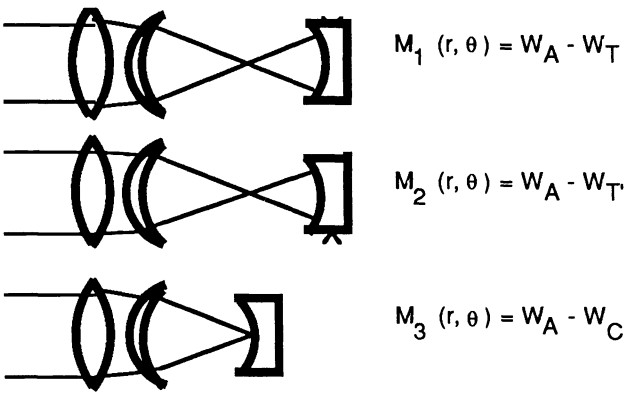

where $W_A(r,\theta)$ is the wavefront reflected from the aplanat,
$W_T(r,\theta)$ is the wavefront reflected from the test surface,
$W_{T'}(r,\theta)$ is the wavefront reflected from the test surface after 180° rotation,
$W_C(r,\theta)$ is the wavefront reflected from the cat's eye reflection.

Figure 2. Spherical Certification Measurements

The absolute measurement of the test surface $T(r,\theta)$ requires three measurements as shown in Fig. 2.

Using Figs. 1 and 2, Eq. (1), and the fact that the aberrations introduced by each element in the optical path add linearly, the results of the measurements can be calculated. First calculate each wavefront component.

$$W_A(r,\theta) = I(r,\theta) + 2\,L(r,\theta) + 2n\,A(r,\theta)\,. \tag{2}$$

$$W_T(r,\theta) = I(r,\theta) + 2\,L(r,\theta) + 2(n-1)\,A(r,\theta) + 2\,T(r,\theta)\,. \tag{3}$$

$$W'_T(r,\theta) = I(r,\theta) + 2\,L(r,\theta) + 2(n-1)\,A(r,\theta) + 2\,T(r,\theta + 180°)\,. \tag{4}$$

$$W_C(r,\theta) = I(r,\theta) + L(r,\theta) + (n-1)\,A(r,\theta) + (n-1)\,A(r,\theta + 180°) + L(r,\theta + 180°)\,. \tag{5}$$

Where $I(r,\theta)$ is the wavefront error of the source,
$L(r,\theta)$ is the wavefront error introduced by the focusing optics in the aplanat,
$A(r,\theta)$ is the error in the aplanat reference surface, and
$T(r,\theta)$ is the error in the surface under test.